Supplementary Resources I:

Latest deep learning-based articles for EEG-based motor imagery classification

The content of this document is part of the following review paper:

Deep learning techniques for classification of electroencephalogram (EEG) motor imagery (MI) signals: a review

https://doi.org/10.1007/s00521-021-06352-5

For the details, the reader can refer to the above paper.

If you use the data in this document, please cite the original review paper as:

H. Altaheri, G. Muhammad, M. Alsulaiman, et al. "Deep learning techniques for classification of electroencephalogram (EEG) motor imagery (MI) signals: a review". Neural Comput. Appl., vol. 35, no. 20, 14681–14722, 2023. https://doi.org/10.1007/s00521-021-06352-5

Summary of the different deep learning models with the input formulation used for motor imagery (MI) classification

		Input Formulation																													
		Extracted features													Spectral images							Raw signal values	Topological maps								
		Temporal features				Frequency features			Time-frequency features					Spatial features	Time-frequency images. *Generated by: E.g., WT, STFT, CWT, MW, ST, QTFD. Represented as: [T × F]^{1}, [T × F × C]^{2}, [T × F+C]^{3} [T+C × F]^{4} [(T+C) × (F+C)]^{5}*						Spatial-frequency images. *FFT energy map: [C × F]^{1}, Energy: [C × F-band]^{2}*	2D matrices *(Segments of time-points) [TP × C] matrices*	Time domain				Spectral domain (Generated by, e.g., CWT, ST, PSD, FFT)				
																							Direct map	Time Segments (average values)		Graph-based	One map			Multiple maps	
Deep Learning Model		SM	NSCM	CorrM	PCA	DCT	FFT	PSD	EMD	HHT	WT	WPD	DWT	CSP	*STFT*	*WT*	*MW*	*CWT*	*ST*	*QTFD*			Time points *(power values) 3D: [2D-map × Time]*	One map	Multiple maps		*ST*	CWT	PSD	FFT	power
CNN			[81]	[66]		[75]		[76]	[9] [75]	[79]	[120]		[76]	[71] [72] [73] [143] [123] [126] [75] [82] [83]	[7]^{1} [90]^{3} [141]^{3} [92]^{3} [93]^{3} [98]^{3} [148]^{1} [130]^{2} [94]^{2}	[65]^{2}	[150]^{2}	[96]^{2} [97]^{4} [146]^{3} [147]^{3} [148]^{1}	[67]^{5}	[68]^{3}	[95]^{2} [89]^{1}	[103] [104] [105] [106] [107] [108] [62] [109] [135] [128] [110] [55] [129] [111] [127] [125] [121] [114] [112]^{A} [140] [57] [113] [122] [124]	[116] [117] [54]^{3D} [58]^{3D}		[118]		[67]	[119]	[119]	[118]	[118]
RNN	LSTM	[80]												[70] [84] [85]	[7]^{1} [90]^{3}																
RNN	GRU													[70]																	
ELM														[74]																	
DSN	DSN-RBM																					[149] [151]									
DBN	DBN-AE						[51]								[98]^{3}																
DBN	DBN-RBM				[86]		[51] [77]	[61]				[77] [78]		[78]																	
Hybrid	CNN+RNN														[7]^{1}																
Hybrid	CNN+GRU																							[59]							
Hybrid	CNN+LSTM													[87] [88]								[137] [138] [63] [56]				[100]^{A}					
Hybrid	CNN+AE														[98]^{3} [99]^{3VA}							[115] [60]									
Hybrid	CNN+MLP																					[115]									
Hybrid	CNN+GAN														[91]^{3}							[64]									
Generative	VAE														[91]^{3} [99]^{3}																
Generative	GAN														[91]^{3}							[64]									

__A__: Attention. Extracted features, __SM__: Statistical measures, __CorrM__: Correlation matrix, __PCA__: Principal component analysis, __NSCM__: normalized sample covariance matrix. Spatial features, __CSP__: Common spatial pattern. Frequency features, __PSD__: Power spectral density, __FFT__: Fast Fourier transform, __DCT__: discrete cosine transform. Time-frequency features, __WT__: Wavelet transform, __DWT__: Discrete wavelet transform, __WPD__: Wavelet packet decomposition, __CWT__: Continuous wavelet transform, __MW__: Morlet wavelets, __STFT__: Short-time Fourier transform, __ST__: Stockwell Transform, __EMD__: Empirical mode decomposition, __HHT__: Hilbert-Huang transform, __QTFD__: quadratic time-frequency distribution, __ST__: Stockwell transform. Image representation, (For details, refer to Figure 10), __T__: Time window (time segment), __TP__: Time point (sampling point), __F__: Frequency, __F-band__: Frequency band, __C__: Channel (electrode). Deep Learning Models, __CNN__: Convolutional neural network, __RNN__ Recurrent neural network, __LSTM__: Long short-term memory, __GRU__: Gated recurrent unit, __MLP__: Multi-layer perceptron, __AE__: Auto-encoder, __RBM__: Restricted Boltzmann machine, __DBN__: Deep belief network, __GAN__: Generative adversarial network, __VAE__: Variational autoencoder, __ELM__: Extreme learning machine, __DSN__: Deep stacking network, Summary of artifact removal strategies used for MI-EEG signals

Artifacts removal approach									
AR: Automatic removal							Manual removal	Without removal	Not specified
ICA	BSS+MRIC	DWT	ASR	AAR	Others (E.g., SW such as BCILAB or EEGLAB)	SF: CAR			
[7] [62] [63] [64]	[147]	[97]	[64]	[68] [66]	[71] [61] [9] [76] [120] [78]	[65] [66] [67] [60]	[116] [137] [126]	[103] [98] [104] [115] [105] [70] [77] [99] [100] [141] [91] [93] [109] [143] [51] [54] [84] [149] [123] [130] [150] [151] [110] [85] [58] [129] [111] [127] [125] [121] [114] [59] [112] [57] [113]	[90] [106] [118] [72] [74] [117] [95] [92] [96] [138] [107] [108] [79] [89] [73] [86] [119] [80] [56] [146] [87] [148] [135] [75] [128] [55] [81] [88] [82] [94] [140] [83]

ICA: *Independent component analysis,* ***DWT***: *Discrete wavelet transform,* ***SF:*** *Spatial filter,* ***CAR***: *Common average reference filter,* ***AAR***: *Automatic artifact removal,* ***ASR***: *Artifact subspace reconstruction,* ***BSS***: *Blind Source Separation,* ***MRIC***: *Movement Related Independent Component,* ***SW***: *software.*

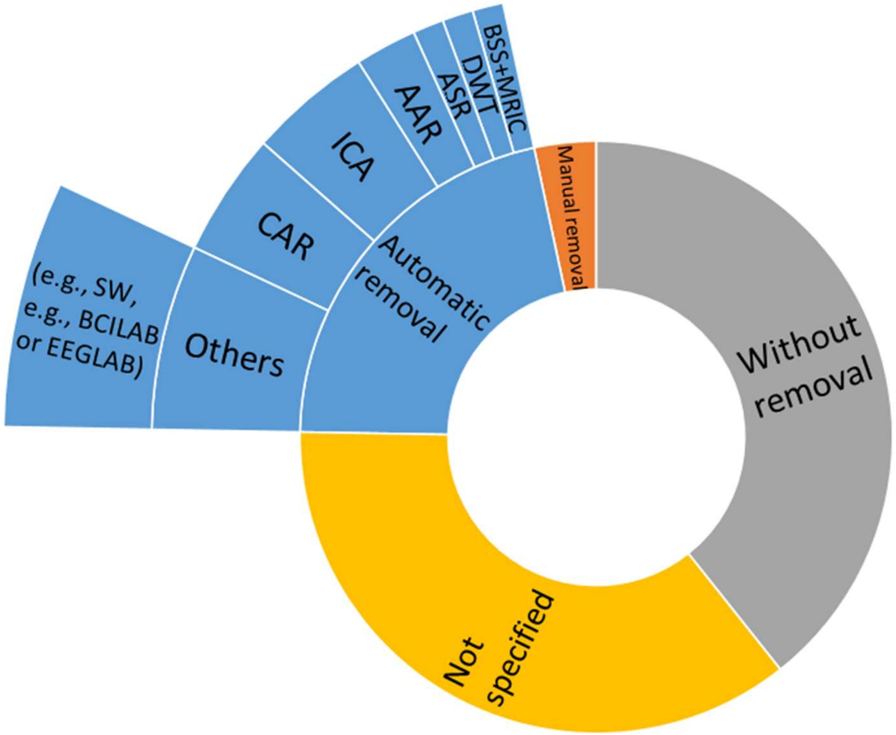

Summary of the latest deep learning-based articles for EEG-based motor imagery classification.

Study	Pre-processing: Selected channels	Pre-processing: Analyzed frequency band (Hz)	Pre-processing: Artifact removal approach	Input formulation*	Deep learning approaches: General strategy	Deep learning approaches: Architecture	Deep learning approaches: Activation function	Dataset	Performance evaluations: Strategy	Performance measures: Accuracy %	Performance measures: kappa	Performance measures: Others (name)
Zhang et al. 2021, [128]	ALL (62)	8-30	N/A	RV: 2D matrices [TP × C]	CNN (adaptive transfer learn.)	5 CONV 1 FC 2 OUT	ELU: conv Smax: L-FC	Lee et al. [50]	sub-d: HO (70: 30) sub-i: CV (LOSO)	sub-d: 63.54±14.25 sub-i: 84.19±9.98	–	Computation time, t-test
Zhang et al. 2021, [114]	ALL (22, 3)	FB (0.5-100)	W	RV: 2D matrices [TP × C]	CNN (inception) (augment: NS)	6×5 CONV 2 FC 4/2 OUT	ReLU: conv N/A: FC Smax: L-FC	DS1: BCI-C IV-2a [131] DS2: BCI-C IV-2b [101]	HO (75 : 25)	DS1: 88.4±7 DS2: 88.6±5	–	CM, ROC, AUC, F-score, TPR
Avilov et al. 2021, [55]	variable (3-128)	4-38	N/A	RV: 2D matrices [TP × C]	CNN	3 CONV 1 FC 2 OUT	ELU: conv Smax: L-FC	Local: 22 sub, 2 MI (presses/releases a button), 128 elec, 1144 trials/class, 2048 Hz.	CV (10 folds)	83.2	–	–
Kumar et al. 2021, [85]	ALL (64)	Adaptive selection	W	EF: CSP	RNN-LSTM +SVM	2 LSTM-L 1 FC 2 OUT	N/A	GigaDB [132]	CV (10 folds)	69.59	0.398	TPR, TNR
Liu et al. 2021, [58]	ALL (22) +variable	FB (0.5-100)	W	TM: TP-3D	CNN (3D) (residual) (multi-branch)	10 CONV 3 FC 4 OUT	ELU: conv ReLU: FC Smax: L-FC	BCI-C IV-2a [131]	CV (10 folds)	81.22 ± 6.85	0.72 ± 0.12	p-value, test/train time
Zhao et al. 2021, [129]	ALL (22, 3)	4-38	W	RV: 2D matrices [TP × C]	CNN (domain adaptation)	2 CONV 3 FC 4/2 OUT	ReLU: conv ReLU: FC sigm: L-FC	DS1: BCI-C IV-2a [131] DS2: BCI-C IV-2b [101]	c-sub: HO DS1: (50:50) DS2: (56:44)	DS1: 74.75 DS2: 83.98	DS1: 0.663 DS2: 0.68	–
Bang et al. 2021, [81]	DS1: 22 DS2: 3 DS3: 20	4-40	N/A	EF: NSCM	CNN (3D)	2 CONV 2 FC 2 OUT	ReLU: conv ReLU: FC N/A: L-FC	DS1: BCI-C IV-2a [131] DS2: BCI-C IV-2b [101] DS3: Lee et al. [50]	CV (10 folds)	DS1: 87.15 DS2: 75.85 DS3: 70.37	–	t-test
Deng et al. 2021, [103]	ALL (22, 60)	4-38	W	RV: 2D matrices [TP × C]	CNN	3 CONV 1 FC 4 OUT	ELU: conv Smax: L-FC	DS1: BCI-C IV-2a [131] DS2: BCI-C III-3a [136]	CV (5 folds)	DS1: 78.96 DS2: 85.30	DS1: 0.72 DS2: 0.80	t-test
Ha et al. 2021, [127]	ALL (22, 3)	4-38	W	RV: 2D matrices [TP × C]	CNN (multi-level pooling)	4 CONV 2 FC 4/2 OUT	ELU: conv ELU: FC Smax: L-FC	DS1: BCI-C IV-2a [131] DS2: BCI-C IV-2b [101]	HO DS1: (50:50) DS2: (56:44)	DS1: 73.19 DS2: 82.83	–	w-test
Zhang et al. 2021, [88]	ALL (22)	4-40	N/A	EF: CSP	Hybrid: CNN/LSTM (transfer learn.)	3 CONV 1 LSTM-L 4 FC 4 OUT	ReLU: conv ReLU: FC Smax: L-FC	BCI-C IV-2b [101]	c-sub: HO (50 : 50)	–	0.81	–
Riyad et al. 2020, [125]	ALL (22)	0-38 4-38	W	RV: 2D matrices [TP × C]	CNN (inception) (augment: SW)	11 CONV 1 FC 4 OUT	ELU: conv Smax: L-FC	BCI-C IV-2b [101]	CV (5 folds)	74.61	0.662	CM
Liu et al. 2020, [121]	ALL (22)	0-38	W	RV: 2D matrices [TP × C]	CNN (self-attention) (transfer learn.)	7 CONV 1 FC 4 OUT	N/A: conv Smax: L-FC	BCI-C IV-2b [101]	c-sub: CV (10 folds) HO (50 : 50)	HO: 78.51 CV: 90.15	–	CM
Xue et al. 2020, [82]	ALL (22, 60)	4-40	N/A	EF: CSP	CNN (multi-layer)	7 CONV 3 FC 4 OUT	ELU: conv ELU: FC Smax: L-FC	DS1: BCI-C IV-2b [101] DS2: BCI-C III-3a [136]	HO (70 : 30)	DS1: 83.83 DS2: 89.45	DS1: 0.78 DS2: 0.86	–
Li et al. 2020, [106]	ALL (22)	8-30	W	RV: 2D matrices [TP × C]	CNN (multi-scale) (attention)	10 CONV 2 FC 4 OUT	ReLU: conv ReLU: FC Smax: L-FC	BCI-C IV-2b [101]	HO (50 : 50)	79.9	–	CM
Li et al. 2020, [59]	ALL (64) +variable	N/A	W	TM: TP (D)	Hybrid: CNN/GRU	3 CONV 1 FC 2 GRU-L 2 FC 4 OUT	N/A: conv N/A: FC Smax: L-FC	EEGMMIDB [139]	HO (75 : 25)	97.36	–	–
Fan et al. 2020, [104]	ALL (64)	0.1-64	W	RV: 2D matrices [TP × C]	CNN (attention) (residual)	14 CONV 1 FC 4 OUT	ReLU: conv N/A: L-FC	EEGMMIDB [139]	CV (5 folds)	65.82	–	CM
Roy et al. 2020, [94]	ALL (3)	4-32	N/A	SI: TFI (STFT) [T × F × C]	CNN	3 CONV 2 FC 2 OUT	ReLU: conv N/A: FC Smax: L-FC	BCI-C IV-2b [101]	sub-d: HO (56 : 44) sub-i: CV (LOSO)	sub-d: 77.5±14.5 sub-i: 70.9±9.9	sub-d: 0.55±0.29 sub-i: 0.42±0.2	–
Xiaoling et al. 2020, [140]	28	8-30	N/A	RV: 2D matrices [TP × C]	CNN	2 CONV 2 FC 2 OUT	tanh: conv sigm: FC sigm: L-FC	Local: 4 sub, 2 MI left-hand/foot, 560 trials/sub, 1000 Hz (1-40 Hz), 64 elec.	HO (80 : 20)	90.08±2.22	–	CM, RC, PR, F-score, ROC, w-test, T-comp
Lun et al. 2020, [57]	2 +variable	N/A	W	RV: 2D matrices [TP × C]	CNN	5 CONV 1 FC 4 OUT	LReLU: conv Smax: L-FC	EEGMMIDB [139]	sub-d: CV (10 folds) sub-i: HO (106: 3 subs)	sub-d: 94.80 sub-i: 72.47	–	CM, RC, PR, F-score, ROC, AUC
Roots et al. 2020, [105]	ALL (64)	2-60	W	RV: 2D matrices [TP × C]	CNN (multi-branch) (augment: SW)	3×3 CONV 1 FC 2 OUT	ELU: conv Smax: L-FC	EEGMMIDB [139]	c-sub HO (80 : 20)	83.8	–	CM, RC, PR, F-score, t-test
Yang et al. 2020, [60]	variable (3-25)	7-35	A: CAR	RV: 2D matrices [TP × C]	Hybrid: CNN/SAE (multi-layer-CNN)	5 CONV 2 AE (1 hid) 1 FC 2 OUT	ReLU: conv Smax: L-FC	DS1: BCI-C IV-1 [133] DS2 (Local): 6 sub, 2 MI L/R hand, 64 elec, 300 trials/sub, 256 Hz.	sub-d: CV (8 folds) sub-i: CV (LOSO)	sub-i: DS1: 86.4 DS2: 84.7	sub-i DS1: 0.45 DS2: 0.46	–
Zhao et al. 2020, [83]	ALL (64, 22)	4-40	N/A	EF: CSP	CNN (domain adaptation)	4 CONV 1 FC 2 OUT	ReLU: conv Smax: L-FC	DS1: GigaDB [132] DS2: BCI-C IV-2a [131]	c-sub: HO (8 : 1 subs) (5 : 1 subs)	N/A	–	–
Zhang et al. 2020, [100]	ALL (64, 22)	FB (DS2: 0.5-100)	W	TM: TP (G)	Hybrid: CNN/LSTM (recurrent attention)	1 CONV 2 LSTM-L 1 FC 4 OUT	ELU: conv Smax: L-FC	DS1: EEGMMIDB [139] DS2: BCI-C IV-2a [131]	sub-i: HO (subs) DS1: (95:10) DS2: (8 : 1)	DS1: 74.2 DS2: 60.1	–	ROC, AUC
Xu et al. 2020, [116]	ALL (22)	9-20 +variable	M	TM: TP (D)	CNN	3 CONV 2 FC 4 OUT	ReLU: conv ReLU: FC Smax: L-FC	BCI-C IV-2a [131]	HO	84.57	0.801	_
Zhang et al. 2020, [141]	ALL (3)	8-30	W	SI: TFI (STFT) [T× F+C]	CNN	2 CONV 2 FC 2 OUT	ReLU: conv Smax: FC Smax: L-FC	BCI-C IV-2b [101]	CV (10 folds)	94.7 ± 2:6	0.664	_
Liao et al. 2020, [117]	ALL (22)	4-40	N/A	TM: TP (D)	CNN	3 CONV 1 FC 4 OUT	LReLU: conv Smax: L-FC	BCI-C IV-2a [131]	HO (50 : 50)	74.60	0.66	_

Zhang et al. 2020, [91]	3	8-30	W	SI: TFI (STFT) [T × F+C]	Hybrid: CNN/GAN (also VAE)	4:4 CONV CNN: 2 CONV 2 FC 2 OUT	LReLU: d-conv ReLU: conv Smax: FC Smax: L-FC	DS1: BCI-C IV-1 [133] DS2: BCI-C IV-2b [101]	CV (10 folds)	DS1: 83.2 ± 3.5 DS2: 93.2 ± 2.8	DS1: 0.468 DS2: 0.671	t-test, p-value
Miao et al. 2020, [95]	49	8–30	N/A	SI: SFI (Energy) [C × F-band]	CNN	2 CONV 3 FC 2 OUT	ReLU: conv ReLU: FC Smax: L-FC	DS1: BCI-C III-4a [136] DS2 (Local): 5 sub, 2 MI finger/rest, 21 elec, 1000 Hz.	CV (10 folds)	DS1: 90.0	–	Running time
Tang et al. 2020, [9]	3	8–30	A	EF: (EMD)	CNN (1D) (multi-scale) (inception)	4 CONV 2 FC 2 OUT	ReLU: conv N/A: FC Smax: L-FC	DS1: BCI-C IV-2b [101] DS2 (Local): 5 sub, 2 MI L/R hand, 14 elec, 128 Hz, 10 s trial.	N/A	DS1: 82.61 DS2: 85.83	–	p-value
Shajil et al. 2020, [92]	5	1-100 13-30	N/A	SI: TFI (STFT) [T× F+C]	CNN	1 CONV 2 FC 4 OUT	ReLU: conv N/A: FC Smax: L-FC	Local: 12 sub, 4 MI (L/R hand, both hands, feet), 16 elec, 500 Hz.	N/A	87.37 ± 1.68	–	–
Xu et al. 2020, [78]	ALL (22)	8-30	A: EEGLAB	EF: WPD, CSP	DBN-RBM (stacked RBM) +SVM	4 RBM (1 hid) 4 OUT	sigm: RBM Linear: last RBM	BCI-C IV-2a [131]	CV (10 folds)	78.51	0.6278	–
Taheri et al. 2020, [75]	1	N/A	N/A	EF: CSP, DCT, EMD	CNN+SVM (multi-branch)	5 CONV 2 FC 2 OUT	ReLU: conv ReLU: FC	BCI-C III-4a [136]	HO (70 : 30)	96.34	–	–
Wang et al. 2020, [137]	ALL (22)	8-30	M	RV: 2D matrices [TP × C]	Hybrid: CNN/LSTM	3 CONV 1 FC 2 LSTM-L 1 FC 4 OUT	ELU/Linaer: conv Smax: L-FC	BCI-C IV-2a [131]	HO (50 : 50)	–	0.64 ± 0.14	t-test
Li et al. 2020, [96]	ALL (3)	4-30	N/A	SI: TFI (CWT) [T×F×C]	CNN	2 CONV 2 FC 2 OUT	ReLU: conv ReLU: FC Smax: L-FC	BCI-C IV-2b [101]	CV (10 folds)	83.2	0.651	–
Rong et al. 2020, [93]	ALL (3)	4-32	W	SI: TFI (STFT) [T× F+C]	CNN	3 CONV 1 FC 2 OUT	ReLU: conv Smax: L-FC	BCI-C IV-2b [101]	HO (90 : 10)	82.8	0.663	–
Ma et al. 2020, [76]	ALL (22)	0.5-50	A	EF: DWT +PSD	CNN	4 CONV 2 FC 4 OUT	ReLU: conv N/A: FC N/A: L-FC	BCI-C IV-2a [131]	CV (8 folds)	96.21	–	test/train time
Hou et al. 2020, [120]	ALL (64)	8-30	A	EF: WT	CNN	6 CONV 2 FC 4 OUT	LReLU: conv LReLU: FC Smax: L-FC	EEGMMIDB [139]	CV (10 folds)	94.5	–	–
Freer et al. 2020, [138]	ALL (22)	7-30	N/A	N/A	Hybrid: CNN/LSTM (augment)	4 CONV 1 LSTM-L 1 FC 4 OUT	ELU: conv Smax: L-FC	BCI-C IV-2a [131]	N/A	–	–	PR, RC
Dai et al. 2020, [111]	3	4-32	N/A	RV: 2D matrices [TP × C]	CNN (multi-layer) (augment)	2 CONV 2 FC 4/2 OUT	ELU: conv N/A: FC N/A: L-FC	DS1: BCI-C IV-2a [131] DS2: BCI-C IV-2b [101]	HO	DS1: 91.57 DS2: 87.6	–	P-values
Lee et al. 2020, [112]	24	4-40	N/A	RV: 2D matrices [TP × C]	CNN (multi-branch)	4 CONV 1 FC 9 OUT	ELU: conv Smax: L-FC	Local: 9 MI, 12 sub, 50 trials/sess, 3 sess, 1000 Hz, 64 elec.	CV (5 folds)	81	–	CM
Huang et al. 2020, [79]	ALL (22)	FB 0.5-100	N/A	EF: HHT	CNN	5 CONV 2 FC 4 OUT	Linear/ReLU: conv N/A: FC Smax: L-FC	BCI-C IV-2a [131]	CV (4 folds)	77.9	–	–
Li et al. 2020, [118]	ALL (64, 22, 3)	8-30	N/A	TM: TP (D)	CNN	31 CONV 1 FC 4/4/2 OUT	ReLU: conv Smax: L-FC	DS1: EEGMMIDB [139] DS2: BCI-C IV-2a [131] DS3: BCI-C IV-2b [101]	DS1,3: CV (10 folds) DS2: HO (50 : 50)	DS1,CV: 89 DS2,HO: 89 DS3,CV: 97	DS1: 0.77 DS2: 0.78 DS3: 0.94	CM, ROC, AUC
Alwasiti et al. 2020, [67]	ALL (64)	2-78	A: CAR	SI: ST [T+C × F+C]	CNN (DenseNet) (deep metric learning)	1 CONV 4 DB 2 FC 3 OUT	ReLU: conv ReLU: DB ReLU: FC Smax: L-FC	EEGMMIDB [139]	HO (80 : 20)	64.7	–	CM, PR, RC
Jeong et al. 2020, [62]	20	4-40	A: ICA	RV: 2D matrices [TP × C]	CNN (multi-layer)	5 CONV 2 FC 3 OUT	ELU: conv ELU: FC Smax: L-FC	DS1: ULMov [142] DS2 (Local): 10 sub, 3 MI (forearm angle), 150 trials, 100 Hz, 32 elec.	HO (80 : 20)	DS1: 51.0 ± 4.0 DS2: 65.0 ± 9.0	–	CM, t-test
Cheng et al. 2020, [86]	ALL	0.5-30	N/A	EF: PCA	DBN-RBM	5 RBM (1 hid) 1 FC 2 OUT	Smax: L-FC	DS1: BCI-C IV-2b [101] DS2: BCI-C II-3 [102]	CV (10 folds)	DS1: 91.71 DS2: 96.25	DS1: 0.8342 DS2: 0.925	t-test, test/train time
Collazos et al. 2020, [119]	ALL (22)	8-30	N/A	TM: SP (CWT, PSD)	CNN (multiple input CNN)	4 CONV 2 FC 3 OUT	ReLU: conv ReLU: FC Smax: L-FC	BCI-C IV-2a [131]	CV (10 folds)	71.2 ± 7.0	0.56	p-values
Chen et al. 2020, [143]	ALL (22, 15)	8-30	W	EF: CSP	CNN	3 CONV 2 FC 4 OUT	ReLU: conv N/A: FC Smax: L-FC	DS1: BCI-C IV-2a [131] DS2: Steyrl et al. [144]	HO (70 : 30)	DS1: 72 DS2: 82.9	DS1: 0.627 DS2: 0.657	CM, t-test
Kant et al. 2020, [97]	ALL (2)	8-30	A: DWT	SI: TFI (CWT) [T+C ×F]	CNN (transfer learning)	14 CONV 4 FC 2 OUT	ReLU: conv ReLU: FC Smax: L-FC	BCI-C II-3 [102]	HO (50 : 50)	95.71	0.91	CM
Fahimi et al. 2020, [64]	ALL	0.5-100	A: ICA, ASR	RV: 2D matrices [TP × C]	Hybrid: CNN/GAN	2:2 CONV 3 CONV 2 FC 2 OUT	tanh: G-conv ReLU: conv ReLU: FC sigm: L-FC	DS1: BCI-C III-4a [136] DS2 (Local): 14 sub, 2 MI open/close R-hand, 62 elec.	HO (50 : 50)	DS1: 71.14	–	–
Ma et al. 2019, [66]	ALL (64)	0.1-40	A: CAR, AAR	EF: CorrM	CNN (multi-branch)	2 CONV 1 FC 3 OUT	ReLU: conv Smax: L-FC	MIJoint [145]	CV (5 folds)	87.03	–	–
Hassanpour et al. 2019, [51]	ALL (22) +variable	8-35	W (+A: SWT)	EF: FFT	DBN-AE DBN-RBM (augment: SW)	5 RBM/AE (1 hid) 1 FC 4 OUT	N/A: AE Smax: L-FC	BCI-C IV-2a [131]	HO (50 : 50)	DBN-AE: 71.0 DBN-RBM: 68.4	–	t-test, train time
Zhu et al. 2019, [56]	variable (3-64)	N/A	N/A	RV: 2D matrices [TP × C]	Hybrid: CNN/LSTM (also CNN)	2 CONV 1 LSTM-L 1 FC 2 OUT	N/A	EEGMMIDB [139]	N/A	82.93 (CNN: 79.7)	–	–
Lee et al. 2019, [146]	ALL (3)	8-30	N/A	SI: TFI (CWT) [T× C+F]	CNN	1 CONV 1 FC 2 OUT	ReLU: conv N/A: L-FC	DS1: BCI-C IV-2b [101] DS2: BCI-C II-3 [102]	CV (10 folds)	DS1: 83.0±1.6 DS2: 92.9	–	–
Zhang et al. 2019, [87]	ALL (22)	4-38	N/A	EF: FBCSP	Hybrid: CNN/LSTM	3 CONV 3 LSTM-L 4 OUT	ReLU: conv Smax: out	BCI-C IV-2a [131]	HO	84	0.81	–

Amin et al. 2019, [115]	ALL (22)	0.5-40	W	RV: 2D matrices [TP × C]	Hybrid: CNN/MLP (M) CNN/AE (A) (multi-layer-CNN)	5 CONV 4 FC MLP (2 hid)/ AE (1 hid) 4 OUT	ELU: conv ELU: AE ELU: MLP N/A: FC Smax: L-FC	BCI-C IV-2a [131]	sub-d: HO (50 : 50) sub-i: CV (LOSO)	sub-d: M: 75, A: 73 sub-i: M: 42, A: 55	–	CM, train time
Wu et al. 2019, [113]	ALL (22, 3)	4-38	W	RV: 2D matrices [TP × C]	CNN	5 CONV 1 FC 4/2/3 OUT	Linear	DS1: BCI-C IV-2a [131] DS2: BCI-C IV-2b [101]	c-sub: HO	DS1: 75.9 DS2: 84.7	–	–
Ortiz et al. 2019, [147]	18	0.5-90	A: BSS+ MRIC	SI: CWT [T × C+F]	CNN	2 CONV 2 FC 2 OUT	ReLU: conv ReLU: FC Smax: L-FC	BCI-C III-4a [136]	CV (10 folds)	94.66	–	–
Zhao et al. 2019, [54]	ALL (22) +variable	0.5-100 +variable	W	TM: TP-3D	CNN (3D) (multi-branch)	3 CONV 3 FC 4 OUT	ELU: conv ReLU: FC Smax: L-FC	BCI-C IV-2a [131]	CV (10 folds)	75.02	0.644	t-test, test/train time
Kumar et al. 2019, [84]	ALL (64, 59)	7-30	W	EF: CSP	RNN-LSTM	2 LSTM-L 1 FC 2 OUT	N/A	DS1: GigaDB [132] DS2: BCI-C IV-1 [133]	CV (10 folds)	DS1: 68.19 DS2: 82.52	DS1: 0.374 DS2: 0.650	TPR, TNR
Chaudhary et al. 2019, [148]	N/A	N/A	N/A	SI: TFI (STFT/CWT) [T × F]	CNN	5 CONV 3 FC 2 OUT	ReLU: conv Smax: FC Smax: L-FC	BCI-C III-4a [136]	HO (80 : 20)	99.35	0.987	TPR, TNR, F-score, CM
Li et al. 2019, [135]	ALL (22)	N/A	N/A	RV: 2D matrices [TP × C]	CNN (augment: AP)	5 CONV 2 FC 4 OUT	ELU: conv ELU: FC Smax: L-FC	BCI-C IV-2a [131]	HO (50 : 50)	74.6	–	CM, PR, RC, F-score, train time
Tang et al. 2019, [149]	DS1: ALL (3) DS2: 6	8-30	W	RV: 2D matrices [TP × C]	DSN-RBM (semi-supervised)	7 RBM (1 hid) 2 OUT	N/A	DS1: BCI-C IV-2b [101] DS2 (Local): 7 sub, 2 MI L/R hand, 128 Hz, 240 trials/sub, 14 elec.	HO	DS1: 83.55	–	p-value, train time
Zhu et al. 2019, [123]	ALL (3, 15)	8-30	W	EF: CSP	CNN (residual)	13 CONV 1 FC 2 OUT	ReLU: conv Smax: L-FC	DS1: BCI-C IV-2b [101] DS2 (Local): 25 sub, 2 MI L/R hand, 1000 Hz, 200 trials/sub, 15 elec.	sub-i CV (LOSO)	DS1: 64.0 DS2: 73.0	–	ITR
Dai et al. 2019, [99]	ALL (3, 5)	6-30	W	SI: TFI (STFT) [T × F+C]	Hybrid: CNN/VAE	1 CONV 5 hid. VAE 2 OUT	ReLU: conv	DS1: BCI-C IV-2b [101] DS2 (Local): 5 sub, 2 MI L/R hand, 400 trials, 3 sess, 250 Hz, 5 elec.	CV (10 folds)	–	DS1: 0.564 DS2: 0.568	p-value, train time
Olivas-Padilla et al. 2019, [71]	8	8-30	A: BCILAB	EF: FBCSP (set as a matrix)	CNN	4 CONV 1 FC 4 OUT	ReLU: conv Smax: L-FC	DS1: BCI-C IV-2a [131] DS2 (Local): 8 sub, 4 MI L/R hand/foot, 5 sess, 120 trials/sess, 250 Hz, 8 elec.	DS1: HO (50 : 50) DS2: CV (10 folds)	DS1: 78.41±5.9 DS2: 73.78±4.2	DS1: 0.59±0.11 DS2: 0.64±0.07	–
Alazrai et al. 2019, [68]	ALL (16)	0.5-32.5	A: AAR	SI: TFI (QTFD) [T× F+C]	CNN+SVM	2 CONV 1 FC 11 OUT	ReLU: conv Smax: L-FC	Local: 11 MI, 22 sub, 2048 Hz, 16 elec.	CV (10 folds)	73.70	–	PR, RC, F-score, train/test time
Li et al. 2019, [126]	ALL (22)	8-30	M	EF: CSP	CNN (multi-layer)	9 CONV 2 FC 4 OUT	ReLU: conv Smax: FC Smax: L-FC	BCI-C IV-2a [131]	HO (50 : 50)	79.9	–	–
Xu et al. 2019, [130]	ALL (3)	4-32	W	SI: TFI (STFT) [T×F×C]	CNN (transfer learning)	13 CONV 3 FC 2 OUT	ReLU: conv ReLU: FC Smax: L-FC	BCI-C IV-2b [101]	HO (80 : 20)	74.2	–	train time
Zhang et al. 2019, [150]	ALL (3, 14)	8-30	W	SI: TFI (WT: MW) [T×F×C]	CNN (augment)	2 CONV 2 FC 2 OUT	ReLU: conv ReLU: FC Smax: L-FC	DS1: BCI-C II-3 [102] DS2 (Local): 5 sub, 2 MI L/R hand, 256 Hz, 120 trials/sub, 14 elec.	CV (5 folds)	DS1: 90.1 DS2: 90.0	–	–
Amin et al. 2019, [108]	ALL (22)	FB (0.5-100)	W	RV: 2D matrices [TP × C]	CNN (multi-layer)	5 CONV 4 FC 1 FC 4 OUT	ELU: conv ELU: FC Smax: L-FC	BCI-C IV-2a [131]	sub-i: CV (LOSO)	74.5	–	CM, PR, RC, train time
Tayeb et al. 2019, [7]	ALL (3)	2-60	A: ICA (FASTER)	SI: TFI (STEF) [T × F]	CNN (also LSTM, and RCNN (CNN\RNN))	3 CONV 1 FC 2 OUT	ReLU: conv Smax: L-FC	DS1: BCI-C IV-2b [101] DS2 (Local-public): 20 sub, 2 MI L/R hand, 2 sess, 4 runs, total 750 trials, 256 Hz, 3 elec.	CV (5 folds)	DS1: CNN: 91.63 DS2: CNN: 84.24 RCNN: 77.7	–	–
Kwon et al. 2019, [73]	20	0-40	N/A	EF: CSP	CNN (multi-branch)	3×3 CONV 2 FC 2 OUT	ReLU: conv N/A: FC Smax: L-FC	Lee et al. [50]	sub-d: HO (50 : 50) sub-i: CV (LOSO)	sub-d: 71.3±15.8 sub-i: 74.2±15.8	–	t-test
Xu et al. 2018, [65]	DS1: 3 (DS2:ALL)	8-30	A: CAR	SI: TFI (WT) [T×F×C]	CNN	2 CONV 2 FC 4/2 OUT	ReLU: conv N/A: FC N/A: L-FC	DS1: BCI-C IV-2a [131] DS2: BCI-C II-3 [102]	CV (5 folds)	DS1: 85.59 DS2: 89.56	DS1: 0.766	F-score, train time
She et al. 2018, [74]	ALL (22)	8-30	N/A	EF: CSP	ELM	3 hid 2 OUT	N/A	BCI-C IV-2a [131]	CV (9 folds)	67.76	0.5701	–
Dose et al. 2018, [109]	ALL (64)	N/A	W	RV: 2D matrices [TP × C]	CNN	2 CONV 1 FC 2/3/4 OUT	ReLU: conv Smax: L-FC	EEGMMIDB [139]	CV (5 folds)	2-class: 80.4 3-class:69.8 4-class:58.6	–	CM, PR, RE, train time
Wang et al. 2018, [90]	3	8-30	N/A	SI: TFI (STFT) [T× F+C]	CNN (also LSTM)	2 CONV 2 FC 2 OUT	SELU: conv N/A: FC Smax: L-FC	Local: 14 sub, 2 MI L/R hand, 60 trials/sub, 256 Hz, 11 elec.	CV (4 folds)	CNN: 92.73 LSTM: 80.2	–	CM, p-value
Sakhavi et al. 2018, [72]	ALL (22)	4-40	N/A	EF: CSP	CNN	3 CONV 1 FC 4 OUT	ReLU: conv Smax: L-FC	BCI-C IV-2a [131]	CV (10 folds)	74.46	0.659	–
Wang et al. 2018, [80]	ALL (22)	FB (0.5-100)	N/A	EF: SM	RNN-LSTM	3 LSTM-L 2 OUT	N/A	BCI-C IV-2a [131]	CV (5 folds)	79.6	–	–
Lawhern et al. 2018, [107]	ALL (22)	4-40	W	RV: 2D matrices [TP × C]	CNN	3 CONV 1 FC 4 OUT	ELU: conv Smax: L-FC	BCI-C IV-2a [131] (128 samples/s)	CV (4 folds)	69	–	AUC
Luo et al. 2018, [70]	ALL (22, 3)	8-30	W	EF: FBCSP (time slices)	RNN-GRU (also RNN-LSTM)	2 GRU-L/ LSTM-L 1 FC 4/2 OUT	N/A	DS1: BCI-C IV-2a [131] DS2: BCI-C IV-2b [101]	HO DS1: (50:50) DS2: (56:44)	GRU: 73.6, 82.8 LSTM: 72.6, 81.5	–	train/test time, complexity, t-test
Chu et al. 2018, [61]	ALL (64)	FB (8-35)	A	EF: PSD (LSP)	DBN-RBM	3 RBM (1 hid) 1 FC 3 OUT	Smax: L-FC	Local: 9 sub, 3 MI L/R hand and foot, 10 runs, 300 trials/sub, 10 s trial, 1000 Hz, 64 elec.	HO (75 : 25)	70.72 ± 2.68	–	–

Yang et al. 2018, [63]	9	N/A	A: ICA	RV: 2D matrices [TP × C]	Hybrid: CNN/LSTM	3 CONV 1 LSTM-L 1 FC 2 OUT	ReLU: conv Smax: L-FC	Local: 2 MI L hand/R foot, 6 sub, 500 Hz, 9 elec.	HO (70 : 30)	86.7	–	ROC, train time
Tang et al. 2017, [151]	DS1: ALL(3) DS2: 6	8-30	W	RV: 2D matrices [TP × C]	DSN-RBM	2 RBM (1 hid) 2 OUT	N/A	DS1: BCI-C IV-2b [101] DS2 (Local): 7 sub, 2 MI L/R hand, 128 Hz, 240 trials/sub, 14 elec.	HO (50 : 50)	DS1: 81.35	–	p-value
Tang et al. 2017, [110]	ALL (28)	8-30	N/A	RV: 2D matrices [TP × C]	CNN	2 CONV 1 FC 2 OUT	tanh: conv sigm: FC sigm: L-FC	Local: 2 sub, 2 MI L/R hand, 460 trials/sub, 1000 Hz, 28 elec.	CV (10 folds)	86.4 ± 0.77	–	CM, PR, RC, F-score
Uktveris et al. 2017, [89]	ALL (22)	7-30	N/A	SI: SFI (FFT) [C × F]	CNN	2 CONV 1 FC 4 OUT	ReLU: conv Smax: L-FC	BCI-C IV-2a [131]	CV (10 folds)	68	–	–
Lu et al. 2016, [77]	ALL (3)	8-35	W	EF: FFT (also WPD)	DBN-RBM	3 RBM (1 hid) 1 FC 2 OUT	Smax: L-FC	BCI-C IV-2b [101]	HO (56 : 44)	84	–	t-test
Tabar et al. 2016, [98]	ALL (3)	6-30	W	SI: TFI (STEF) [T × F+C]	Hybrid: CNN/SAE (also, CNN, SAE)	1 CONV 6 AE (1 hid) 1 FC 2 OUT	ReLU: conv sigm: AE N/A: FC	DS1: BCI-C IV-2b [101] DS2: BCI-C II-3 [102]	DS1: CV (10 folds) DS2: HO (50 : 50)	DS1: 77.6 ± 2.1 DS2: 90.0	DS1: 0.55 DS2: 0.80	–

Pre-processing, *Selected channels*, ***ALL:*** *All dataset channels*, ***variable:*** *varying numbers of channels. Analyzed frequency band*, ***FB***: *full-bandwidth in the dataset (0–frequency-end). Artifact removal approach*, ***W***: *Without*, ***M***: *Manual*, ***A***: *Automatic [**ICA**: Independent component analysis, **DWT**: Discrete wavelet transform, **CAR**: Common average reference filter, **AAR**: Automatic artifact removal toolbox, **ASR**: Artifact subspace reconstruction, **BSS**: Blind source separation, **MRIC**: Movement related independent component, **SWT**: Synchrosqueezed wavelet transforms].*

Input formulation, *(* refer to Figure 10), **RV**: Raw values, **EF**: Extracted features [Frequency features [**FFT**: Fast Fourier transform, **DCT**: Discrete cosine transform, **PSD**: Power spectral density [**LSP**: Lomb-Scargle periodogram]], Time-frequency features [**EMD**: Empirical mode decomposition, **HHT**: Hilbert-Huang transform, **WT**: Wavelet transform, **DWT**: Discrete wavelet transform, **WPD**: Wavelet packet decomposition], Spatial features [**CSP**: Common spatial pattern, **FBCSP**: Filter bank CSP], **NSCM**: Normalized sample covariance matrix, **SM**: Statistical measures, **CorrM**: Correlation matrix, **PCA**: Principal component analysis], **SI**: Spectral images [**TFI**: Time-frequency images [**ST**: Stockwell transform, **QTFD**: Quadratic time-frequency distribution, WT [**CWT**: Continuous wavelet transform, **MW**: Morlet wavelets], **STFT**: Short-time Fourier transform], **SFI**: Spatial-frequency images], **TM**: Topological maps [**TP**: Time-domain point [**D**: Direct map, **G**: Graph-based], **SP**: Spectral-domain power].**T**: Time window (time segment), **TP**: Time point (sampling point), **F**: Frequency, **F-band**: Frequency band, **C**: Channel (electrode).*

Deep learning approaches, *General strategy, CNN, RNN [GRU, LSTM], MLP, RBM, AE, DBN [DBN-RBM, DBN-AE], ELM, **DSN**: Deep stacking network [DSN-RBM], GAN, VAE, Hybrid [CNN/LSTM, CNN/GRU, CNN/MLP, CNN/AE, CNN/VAE, CNN/GAN], SVM, **multi-layer**: multi-layer technique (for CNNs), **multi-branch**: multiple branches of CNNs (Ensemble learning), **augment**: data augmentation, **SW**: Sliding window, **NS**: Noise addition, **AP**: amplitude-perturbation. Architectures: **CONV**: Convolutional layer, **FC**: Fully connected layer, **DB**: Dense block, **LSTM-L:** LSTM layer, **GRU-L**: GRU layer, **hid**: hidden layer, **OUT**: number of (output) classes. Activation function, **ReLU**: Rectified linear unit, **LReLU**: Leaky rectified linear unit, **ELU**: Exponential linear unit, **SELU**: Scaled exponential linear unit, **tanh**: hyperbolic tangent, **sigm**: Sigmoid, **Smax**: Softmax function, **Linear**: Linear function, **L-FC**: Last fully connected layer, **G-conv, d-conv**: Convolution layer in a (generator/discriminant generator) model.*

Dataset, ***Local****: Private dataset (not available), **sub**: Subjects, **elec**: Electrode, **L/R**: left/right, **sess**: Session, "**x s trial**": Trial duration is x seconds.*

Evaluation Strategy, ***HO****: Hold-out (train: test), **CV**: Cross-validation, **LOSO**: leave-one-subject-out, **c-sub**: Cross-subject, **sub-d**: Subject-dependent, **sub-i**: Subject-independent, **CM**: Confusion matrix, **PR**: Precision (PPV), **RC**: Recall (True negative rate (TPR)/sensitivity), **TNR**: True negative rate (specificity), **ITR**: Information transfer rate, **ROC**: Receiver operating characteristic curve, **AUC**: Area under the curve, **T-comp**: Time complexity, **w-test**: Wilcoxon test, "**(x : y subs)**": x subjects for training and y subjects for testing.*

A visualization of the classification accuracy of EEG-based motor imagery (MI) reported by the latest deep learning-based articles for all public MI datasets.

***HO**: Hold-out (train: test), **CV**: Cross-validation, **LOSO**: Leave-one-subject-out, **c-sub**: Cross-subject, **sub-d**: Subject-dependent, **sub-i**: Subject-independent, **sb**: subjects, **"(x : y sb)"**: x subjects for training and y subjects for testing*

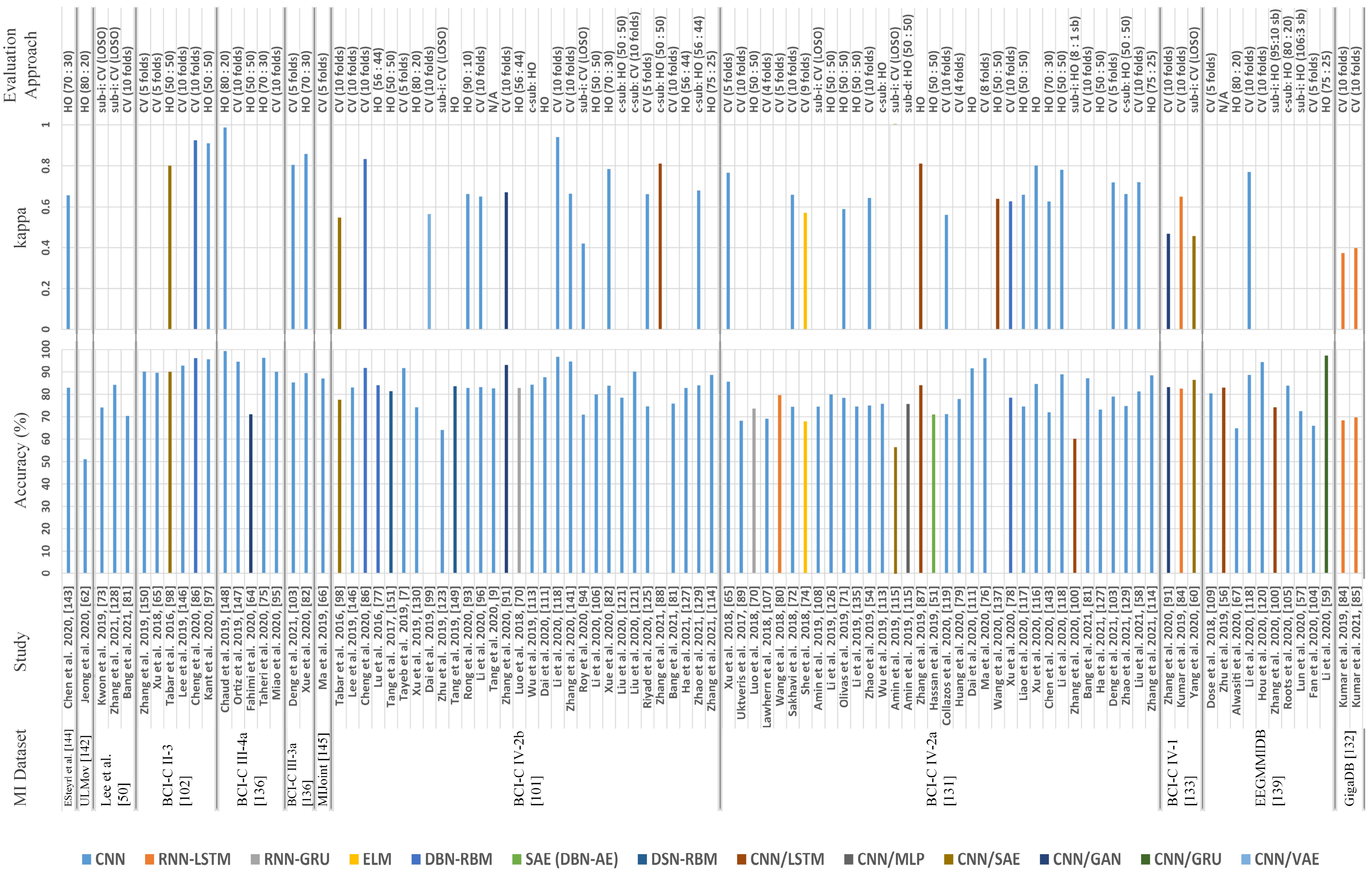

References

[1] F. Alshehri and G. Muhammad, "A comprehensive survey of the Internet of Things (IoT) and AI-based smart healthcare," *IEEE ACCESS*, vol. 9, pp. 3660–3678, 2021.

[2] M. Masud *et al.*, "A lightweight and robust secure key establishment protocol for internet of medical things in COVID-19 patients care," *IEEE Internet Things J.*, 2020.

[3] G. Muhammad, F. Alshehri, F. Karray, A. El Saddik, M. Alsulaiman, and T. H. Falk, "A comprehensive survey on multimodal medical signals fusion for smart healthcare systems," *Inf. Fusion*, 2021.

[4] J. Cantillo-Negrete, R. I. Carino-Escobar, P. Carrillo-Mora, D. Elias-Vinas, and J. Gutierrez-Martinez, "Motor imagery-based brain-computer interface coupled to a robotic hand orthosis aimed for neurorehabilitation of stroke patients," *J. Healthc. Eng.*, vol. 2018, 2018.

[5] E. López-Larraz, A. Sarasola-Sanz, N. Irastorza-Landa, N. Birbaumer, and A. Ramos-Murguialday, "Brain-machine interfaces for rehabilitation in stroke: A review," *NeuroRehabilitation*, vol. 43, no. 1, pp. 77–97, 2018.

[6] M. S. Al-Quraishi, I. Elamvazuthi, S. A. Daud, S. Parasuraman, and A. Borboni, "EEG-based control for upper and lower limb exoskeletons and prostheses: A systematic review," *Sensors*, vol. 18, no. 10, p. 3342, 2018.

[7] Z. Tayeb *et al.*, "Validating deep neural networks for online decoding of motor imagery movements from EEG signals," *Sensors*, vol. 19, no. 1, p. 210, 2019.

[8] Á. Fernández-Rodríguez, F. Velasco-Álvarez, and R. Ron-Angevin, "Review of real brain-controlled wheelchairs," *J. Neural Eng.*, vol. 13, no. 6, p. 61001, 2016.

[9] X. Tang, W. Li, X. Li, W. Ma, and X. Dang, "Motor imagery EEG recognition based on conditional optimization empirical mode decomposition and multi-scale convolutional neural network," *Expert Syst. Appl.*, vol. 149, p. 113285, 2020.

[10] J. Li, J. Liang, Q. Zhao, J. Li, K. Hong, and L. Zhang, "Design of assistive wheelchair system directly steered by human thoughts," *Int. J. Neural Syst.*, vol. 23, no. 03, p. 1350013, 2013.

[11] L. Cao, B. Xia, O. Maysam, J. Li, H. Xie, and N. Birbaumer, "A synchronous motor imagery based neural physiological paradigm for brain computer interface speller," *Front. Hum. Neurosci.*, vol. 11, p. 274, 2017.

[12] D. Das Chakladar and S. Chakraborty, "Multi-target way of cursor movement in brain computer interface using unsupervised learning," *Biol. Inspired Cogn. Archit.*, vol. 25, pp. 88–100, 2018.

[13] A. Delorme, T. Sejnowski, and S. Makeig, "Enhanced detection of artifacts in EEG data using higher-order statistics and independent component analysis," *Neuroimage*, vol. 34, no. 4, pp. 1443–1449, 2007.

[14] A. Jafarifarmand and M. A. Badamchizadeh, "EEG artifacts handling in a real practical brain–computer interface controlled vehicle," *IEEE Trans. Neural Syst. Rehabil. Eng.*, vol. 27, no. 6, pp. 1200–1208, 2019.

[15] D. Pawar and S. Dhage, "Feature Extraction Methods for Electroencephalography based Brain-Computer Interface: A Review.," *IAENG Int. J. Comput. Sci.*, vol. 47, no. 3, 2020.

[16] E. C. Djamal, M. Y. Abdullah, and F. Renaldi, "Brain computer interface game controlling using fast fourier transform and learning vector quantization," *J. Telecommun. Electron. Comput. Eng.*, vol. 9, no. 2–5, pp. 71–74, 2017.

[17] M. R. N. Kousarrizi, A. A. Ghanbari, M. Teshnehlab, M. A. Shorehdeli, and A. Gharaviri, "Feature extraction and classification of EEG signals using Wavelet transform, SVM and artificial neural networks for brain computer interfaces," in *2009 International Joint Conference on Bioinformatics, Systems Biology and Intelligent Computing*, 2009, pp. 352–355.

[18] L. Wang, Z. Lan, Q. Wang, R. Yang, and H. Li, "ELM_Kernel and Wavelet Packet Decomposition Based EEG Classification Algorithm," *Autom. Control Comput. Sci.*, vol. 53, no. 5, pp. 452–460, 2019.

[19] H. Ramoser, J. Muller-Gerking, and G. Pfurtscheller, "Optimal spatial filtering of single trial EEG during imagined hand movement," *IEEE Trans. Rehabil. Eng.*, vol. 8, no. 4, pp. 441–446, 2000.

[20] L. Zhang, D. Wen, C. Li, and R. Zhu, "Ensemble classifier based on optimized extreme learning machine for motor imagery classification," *J. Neural Eng.*, vol. 17, no. 2, p. 26004, 2020.

[21] K. Wang, D.-H. Zhai, and Y. Xia, "Motor Imagination EEG Recognition Algorithm based on DWT, CSP and Extreme Learning Machine," in *2019 Chinese Control Conference (CCC)*, 2019, pp. 4590–4595.

[22] Z. Jin, G. Zhou, D. Gao, and Y. Zhang, "EEG classification using sparse Bayesian extreme learning machine for brain–computer interface," *Neural Comput. Appl.*, pp. 1–9, 2018.

[23] K. K. Ang, Z. Y. Chin, C. Wang, C. Guan, and H. Zhang, "Filter bank common spatial pattern algorithm on BCI competition IV datasets 2a and 2b," *Front. Neurosci.*, vol. 6, p. 39, 2012.

[24] C.-Y. Chen, C.-W. Wu, C.-T. Lin, and S.-A. Chen, "A novel classification method for motor imagery based on Brain-Computer Interface," in *2014 International Joint Conference on Neural Networks (IJCNN)*, 2014, pp. 4099–4102.

[25] M. Arvaneh, C. Guan, K. K. Ang, and C. Quek, "Optimizing the channel selection and classification accuracy in EEG-based BCI," *IEEE Trans. Biomed. Eng.*, vol. 58, no. 6, pp. 1865–1873, 2011.

[26] W. Samek, C. Vidaurre, K.-R. Müller, and M. Kawanabe, "Stationary common spatial patterns for brain–computer interfacing," *J. Neural Eng.*, vol. 9, no. 2, p. 26013, 2012.

[27] W. Samek, M. Kawanabe, and K.-R. Müller, "Divergence-based framework for common spatial patterns algorithms," *IEEE Rev. Biomed. Eng.*, vol. 7, pp. 50–72, 2013.

[28] W. Wu, Z. Chen, X. Gao, Y. Li, E. N. Brown, and S. Gao, "Probabilistic common spatial patterns for multichannel EEG analysis," *IEEE Trans. Pattern Anal. Mach. Intell.*, vol. 37, no. 3, pp. 639–653, 2014.

[29] M. Rashid *et al.*, "Current Status, Challenges, and Possible Solutions of EEG-Based Brain-Computer Interface: A Comprehensive Review," *Front. Neurorobot.*, 2020.

[30] X. Zhang, L. Yao, X. Wang, J. J. M. Monaghan, D. Mcalpine, and Y. Zhang, "A survey on deep learning-based non-invasive brain signals: recent advances and new frontiers," *J. Neural Eng.*, 2020.

[31] H. Altaheri, M. Alsulaiman, and G. Muhammad, "Date Fruit Classification for Robotic Harvesting in a Natural Environment Using Deep Learning," *IEEE Access*, vol. 7, no. 1, pp. 117115–117133, Aug. 2019.

[32] M. Qamhan, H. Altaheri, A. H. Meftah, G. Muhammad, and Y. A. Alotaibi, "Digital Audio Forensics: Microphone and Environment Classification Using Deep Learning," *IEEE Access*, vol. 9, pp. 62719–62733, 2021.

[33] G. Muhammad, M. S. Hossain, and N. Kumar, "EEG-based pathology detection for home health monitoring," *IEEE J. Sel. Areas Commun.*, vol. 39, no. 2, pp. 603–610, 2020.

[34] G. Muhammad, M. F. Alhamid, and X. Long, "Computing and processing on the edge: Smart pathology detection for connected healthcare," *IEEE Netw.*, vol. 33, no. 6, pp. 44–49, 2019.

[35] G. Muhammad, S. K. M. M. Rahman, A. Alelaiwi, and A. Alamri, "Smart health solution integrating IoT and cloud: A case study of voice pathology monitoring," *IEEE Commun. Mag.*, vol. 55, no. 1, pp. 69–73, 2017.

[36] F. Lotte *et al.*, "A review of classification algorithms for EEG-based brain–computer interfaces: a 10 year update," *J. Neural Eng.*, vol. 15, no. 3, p. 31005, 2018.

[37] A. Craik, Y. He, and J. L. Contreras-Vidal, "Deep learning for electroencephalogram (EEG) classification tasks: a review," *J. Neural Eng.*, vol. 16, no. 3, p. 31001, 2019.

[38] N. Padfield, J. Zabalza, H. Zhao, V. Masero, and J. Ren, "EEG-based brain-computer interfaces using motor-imagery: Techniques and challenges," *Sensors*, vol. 19, no. 6, p. 1423, 2019.

[39] S. Aggarwal and N. Chugh, "Signal processing techniques for motor imagery brain computer interface: A review," *Array*, vol. 1, p. 100003, 2019.

[40] Z. Wan, R. Yang, M. Huang, N. Zeng, and X. Liu, "A review on transfer learning in EEG signal analysis," *Neurocomputing*, vol. 421, pp. 1–14, 2020.

[41] E. Lashgari, D. Liang, and U. Maoz, "Data augmentation for deep-learning-based electroencephalography," *J. Neurosci. Methods*, p. 108885, 2020.

[42] D. Moher, A. Liberati, J. Tetzlaff, D. G. Altman, and P. Group, "Preferred reporting items for systematic reviews and meta-analyses: the PRISMA statement," *PLoS med*, vol. 6, no. 7, p. e1000097, 2009.

[43] J. del R. Millán *et al.*, "Combining brain–computer interfaces and assistive technologies: state-of-the-art and challenges," *Front. Neurosci.*, vol. 4, p. 161, 2010.

[44] L. J. Greenfield, J. D. Geyer, and P. R. Carney, *Reading EEGs: A practical approach*. Lippincott Williams & Wilkins, 2012.

[45] T. Ball, M. Kern, I. Mutschler, A. Aertsen, and A. Schulze-

Bonhage, "Signal quality of simultaneously recorded invasive and non-invasive EEG," *Neuroimage*, vol. 46, no. 3, pp. 708–716, 2009.
[46] E. R. Kandel, J. H. Schwartz, T. M. Jessell, S. Siegelbaum, A. J. Hudspeth, and S. Mack, *Principles of neural science*, vol. 4. McGraw-hill New York, 2000.
[47] "CHB-MIT Scalp EEG Database." [Online]. Available: https://archive.physionet.org/physiobank/charts/chbmit.png. [Accessed: 12-Apr-2020].
[48] S. Lacey and R. Lawson, *Multisensory imagery*. Springer Science & Business Media, 2013.
[49] A. Rezeika, M. Benda, P. Stawicki, F. Gembler, A. Saboor, and I. Volosyak, "Brain–computer interface spellers: A review," *Brain Sci.*, vol. 8, no. 4, p. 57, 2018.
[50] M.-H. Lee *et al.*, "EEG dataset and OpenBMI toolbox for three BCI paradigms: an investigation into BCI illiteracy," *Gigascience*, vol. 8, no. 5, p. giz002, 2019.
[51] A. Hassanpour, M. Moradikia, H. Adeli, S. R. Khayami, and P. Shamsinejadbabaki, "A novel end-to-end deep learning scheme for classifying multi-class motor imagery electroencephalography signals," *Expert Syst.*, vol. 36, no. 6, p. e12494, 2019.
[52] G. Pfurtscheller, C. Brunner, A. Schlögl, and F. H. L. Da Silva, "Mu rhythm (de) synchronization and EEG single-trial classification of different motor imagery tasks," *Neuroimage*, vol. 31, no. 1, pp. 153–159, 2006.
[53] Y. Wang, M. Nakanishi, and D. Zhang, "EEG-Based Brain-Computer Interfaces," in *Neural Interface: Frontiers and Applications*, Springer, 2019, pp. 41–65.
[54] X. Zhao, H. Zhang, G. Zhu, F. You, S. Kuang, and L. Sun, "A multi-branch 3D convolutional neural network for EEG-based motor imagery classification," *IEEE Trans. Neural Syst. Rehabil. Eng.*, vol. 27, no. 10, pp. 2164–2177, 2019.
[55] O. Avilov, S. Rimbert, A. Popov, and L. Bougrain, "Optimizing Motor Intention Detection with Deep Learning: Towards Management of Intraoperative Awareness," *IEEE Trans. Biomed. Eng.*, 2021.
[56] K. Zhu, S. Wang, D. Zheng, and M. Dai, "Study on the effect of different electrode channel combinations of motor imagery eeg signals on classification accuracy," *J. Eng.*, vol. 2019, no. 23, pp. 8641–8645, 2019.
[57] X. Lun, Z. Yu, T. Chen, F. Wang, and Y. Hou, "A simplified CNN classification method for MI-EEG via the electrode pairs signals," *Front. Hum. Neurosci.*, vol. 14, 2020.
[58] T. Liu and D. Yang, "A Densely Connected Multi-Branch 3D Convolutional Neural Network for Motor Imagery EEG Decoding," *Brain Sci.*, vol. 11, no. 2, p. 197, 2021.
[59] Y. Li, H. Yang, J. Li, D. Chen, and M. Du, "EEG-based intention recognition with deep recurrent-convolution neural network: Performance and channel selection by Grad-CAM," *Neurocomputing*, vol. 415, pp. 225–233, 2020.
[60] J. Yang, Z. Ma, J. Wang, and Y. Fu, "A Novel Deep Learning Scheme for Motor Imagery EEG Decoding Based on Spatial Representation Fusion," *IEEE Access*, vol. 8, pp. 202100–202110, 2020.
[61] Y. Chu, X. Zhao, Y. Zou, W. Xu, J. Han, and Y. Zhao, "A decoding scheme for incomplete motor imagery EEG with deep belief network," *Front. Neurosci.*, vol. 12, p. 680, 2018.
[62] J.-H. Jeong, B.-H. Lee, D.-H. Lee, Y.-D. Yun, and S.-W. Lee, "EEG classification of forearm movement imagery using a hierarchical flow convolutional neural network," *IEEE Access*, vol. 8, pp. 66941–66950, 2020.
[63] J. Yang, S. Yao, and J. Wang, "Deep fusion feature learning network for MI-EEG classification," *IEEE Access*, vol. 6, pp. 79050–79059, 2018.
[64] F. Fahimi, S. Dosen, K. K. Ang, N. Mrachacz-Kersting, and C. Guan, "Generative Adversarial Networks-Based Data Augmentation for Brain-Computer Interface," *IEEE Trans. neural networks Learn. Syst.*, 2020.
[65] B. Xu *et al.*, "Wavelet transform time-frequency image and convolutional network-based motor imagery EEG classification," *IEEE Access*, vol. 7, pp. 6084–6093, 2018.
[66] X. Ma, S. Qiu, W. Wei, S. Wang, and H. He, "Deep Channel-Correlation Network for Motor Imagery Decoding From the Same Limb," *IEEE Trans. Neural Syst. Rehabil. Eng.*, vol. 28, no. 1, pp. 297–306, 2019.
[67] H. Alwasiti, M. Z. Yusoff, and K. Raza, "Motor imagery classification for brain computer interface using deep metric learning," *IEEE Access*, vol. 8, pp. 109949–109963, 2020.
[68] R. Alazrai, M. Abuhijleh, H. Alwanni, and M. I. Daoud, "A deep learning framework for decoding motor imagery tasks of the same hand using eeg signals," *IEEE Access*, vol. 7, pp. 109612–109627, 2019.
[69] G. Gómez-Herrero *et al.*, "Automatic removal of ocular artifacts in the EEG without an EOG reference channel," in *Proceedings of the 7th Nordic Signal Processing Symposium-NORSIG 2006*, 2006, pp. 130–133.
[70] T. Luo and F. Chao, "Exploring spatial-frequency-sequential relationships for motor imagery classification with recurrent neural network," *BMC Bioinformatics*, vol. 19, no. 1, p. 344, 2018.
[71] B. E. Olivas-Padilla and M. I. Chacon-Murguia, "Classification of multiple motor imagery using deep convolutional neural networks and spatial filters," *Appl. Soft Comput.*, vol. 75, pp. 461–472, 2019.
[72] S. Sakhavi, C. Guan, and S. Yan, "Learning temporal information for brain-computer interface using convolutional neural networks," *IEEE Trans. neural networks Learn. Syst.*, vol. 29, no. 11, pp. 5619–5629, 2018.
[73] O.-Y. Kwon, M.-H. Lee, C. Guan, and S.-W. Lee, "Subject-independent brain–computer interfaces based on deep convolutional neural networks," *IEEE Trans. neural networks Learn. Syst.*, vol. 31, no. 10, pp. 3839–3852, 2019.
[74] Q. She, B. Hu, Z. Luo, T. Nguyen, and Y. Zhang, "A hierarchical semi-supervised extreme learning machine method for EEG recognition," *Med. Biol. Eng. Comput.*, vol. 57, no. 1, pp. 147–157, 2018.
[75] S. Taheri, M. Ezoji, and S. M. Sakhaei, "Convolutional neural network based features for motor imagery EEG signals classification in brain–computer interface system," *SN Appl. Sci.*, vol. 2, no. 4, pp. 1–12, 2020.
[76] X. Ma, D. Wang, D. Liu, and J. Yang, "DWT and CNN based multi-class motor imagery electroencephalographic signal recognition," *J. Neural Eng.*, vol. 17, no. 1, p. 16073, 2020.
[77] N. Lu, T. Li, X. Ren, and H. Miao, "A deep learning scheme for motor imagery classification based on restricted Boltzmann machines," *IEEE Trans. neural Syst. Rehabil. Eng.*, vol. 25, no. 6, pp. 566–576, 2016.
[78] J. Xu, H. Zheng, J. Wang, D. Li, and X. Fang, "Recognition of EEG signal motor imagery intention based on deep multi-view feature learning," *Sensors*, vol. 20, no. 12, p. 3496, 2020.
[79] W. Huang, Y. Xue, L. Hu, and H. Liuli, "S-EEGNet: Electroencephalogram Signal Classification Based on a Separable Convolution Neural Network With Bilinear Interpolation," *IEEE Access*, vol. 8, pp. 131636–131646, 2020.
[80] P. Wang, A. Jiang, X. Liu, J. Shang, and L. Zhang, "LSTM-based EEG classification in motor imagery tasks," *IEEE Trans. neural Syst. Rehabil. Eng.*, vol. 26, no. 11, pp. 2086–2095, 2018.
[81] J.-S. Bang, M.-H. Lee, S. Fazli, C. Guan, and S.-W. Lee, "Spatio-spectral feature representation for motor imagery classification using convolutional neural networks," *IEEE Trans. Neural Networks Learn. Syst.*, 2021.
[82] J. Xue *et al.*, "A Multifrequency Brain Network-Based Deep Learning Framework for Motor Imagery Decoding," *Neural Plast.*, vol. 2020, 2020.
[83] X. Zhao, J. Zhao, C. Liu, and W. Cai, "Deep neural network with joint distribution matching for cross-subject motor imagery brain-computer interfaces," *Biomed Res. Int.*, vol. 2020, 2020.
[84] S. Kumar, A. Sharma, and T. Tsunoda, "Brain wave classification using long short-term memory network based OPTICAL predictor," *Sci. Rep.*, vol. 9, no. 1, pp. 1–13, 2019.
[85] S. Kumar, R. Sharma, and A. Sharma, "OPTICAL+: a frequency-based deep learning scheme for recognizing brain wave signals," *PeerJ Comput. Sci.*, vol. 7, p. e375, 2021.
[86] L. Cheng, D. Li, G. Yu, Z. Zhang, X. Li, and S. Yu, "A Motor Imagery EEG Feature Extraction Method Based on Energy Principal Component Analysis and Deep Belief Networks," *IEEE Access*, vol. 8, pp. 21453–21472, 2020.
[87] R. Zhang, Q. Zong, L. Dou, and X. Zhao, "A novel hybrid deep learning scheme for four-class motor imagery classification," *J. Neural Eng.*, vol. 16, no. 6, p. 66004, 2019.
[88] R. Zhang, Q. Zong, L. Dou, X. Zhao, Y. Tang, and Z. Li, "Hybrid deep neural network using transfer learning for EEG motor imagery decoding," *Biomed. Signal Process. Control*, vol. 63, p. 102144, 2021.
[89] T. Uktveris and V. Jusas, "Application of convolutional neural networks to four-class motor imagery classification problem," *Inf. Technol. Control*, vol. 46, no. 2, pp. 260–273, 2017.
[90] Z. Wang, L. Cao, Z. Zhang, X. Gong, Y. Sun, and H. Wang, "Short time Fourier transformation and deep neural networks for motor

imagery brain computer interface recognition," *Concurr. Comput. Pract. Exp.*, vol. 30, no. 23, p. e4413, 2018.

[91] K. Zhang *et al.*, "Data augmentation for motor imagery signal classification based on a hybrid neural network," *Sensors*, vol. 20, no. 16, p. 4485, 2020.

[92] N. Shajil, S. Mohan, P. Srinivasan, J. Arivudaiyanambi, and A. A. Murrugesan, "Multiclass Classification of Spatially Filtered Motor Imagery EEG Signals Using Convolutional Neural Network for BCI Based Applications," *J. Med. Biol. Eng.*, vol. 40, no. 5, pp. 663–672, 2020.

[93] Y. Rong, X. Wu, and Y. Zhang, "Classification of motor imagery electroencephalography signals using continuous small convolutional neural network," *Int. J. Imaging Syst. Technol.*, vol. 30, no. 3, pp. 653–659, 2020.

[94] S. Roy, A. Chowdhury, K. McCreadie, and G. Prasad, "Deep learning based inter-subject continuous decoding of motor imagery for practical brain-computer interfaces," *Front. Neurosci.*, vol. 14, 2020.

[95] M. Miao, W. Hu, H. Yin, and K. Zhang, "Spatial-frequency feature learning and classification of motor imagery EEG based on deep convolution neural network," *Comput. Math. Methods Med.*, vol. 2020, 2020.

[96] F. Li, F. He, F. Wang, D. Zhang, Y. Xia, and X. Li, "A novel simplified convolutional neural network classification algorithm of motor imagery EEG signals based on deep learning," *Appl. Sci.*, vol. 10, no. 5, p. 1605, 2020.

[97] P. Kant, S. H. Laskar, J. Hazarika, and R. Mahamune, "CWT Based Transfer Learning for Motor Imagery Classification for Brain computer Interfaces," *J. Neurosci. Methods*, vol. 345, p. 108886, 2020.

[98] Y. R. Tabar and U. Halici, "A novel deep learning approach for classification of EEG motor imagery signals," *J. Neural Eng.*, vol. 14, no. 1, p. 16003, 2016.

[99] M. Dai, D. Zheng, R. Na, S. Wang, and S. Zhang, "EEG classification of motor imagery using a novel deep learning framework," *Sensors*, vol. 19, no. 3, p. 551, 2019.

[100] D. Zhang, K. Chen, D. Jian, and L. Yao, "Motor imagery classification via temporal attention cues of graph embedded EEG signals," *IEEE J. Biomed. Heal. informatics*, vol. 24, no. 9, pp. 2570–2579, 2020.

[101] R. Leeb, C. Brunner, G. Müller-Putz, A. Schlögl, and G. Pfurtscheller, "BCI Competition 2008–Graz data set B," *Inst. Knowl. Discov. Graz Univ. Technol.*, pp. 1–6, 2008.

[102] B. Blankertz *et al.*, "The BCI competition 2003: progress and perspectives in detection and discrimination of EEG single trials," *IEEE Trans. Biomed. Eng.*, vol. 51, no. 6, pp. 1044–1051, 2004.

[103] X. Deng, B. Zhang, N. Yu, K. Liu, and K. Sun, "Advanced TSGL-EEGNet for Motor Imagery EEG-Based Brain-Computer Interfaces," *IEEE Access*, vol. 9, pp. 25118–25130, 2021.

[104] C.-C. Fan, H. Yang, Z.-G. Hou, Z.-L. Ni, S. Chen, and Z. Fang, "Bilinear neural network with 3-D attention for brain decoding of motor imagery movements from the human EEG," *Cogn. Neurodyn.*, vol. 15, no. 1, pp. 181–189, 2021.

[105] K. Roots, Y. Muhammad, and N. Muhammad, "Fusion Convolutional Neural Network for Cross-Subject EEG Motor Imagery Classification," *Computers*, vol. 9, no. 3, p. 72, 2020.

[106] D. Li, J. Xu, J. Wang, X. Fang, and J. Ying, "A Multi-Scale Fusion Convolutional Neural Network based on Attention Mechanism for the Visualization Analysis of EEG Signals Decoding," *IEEE Trans. Neural Syst. Rehabil. Eng.*, 2020.

[107] V. J. Lawhern, A. J. Solon, N. R. Waytowich, S. M. Gordon, C. P. Hung, and B. J. Lance, "EEGNet: a compact convolutional neural network for EEG-based brain–computer interfaces," *J. Neural Eng.*, vol. 15, no. 5, p. 56013, 2018.

[108] S. U. Amin, M. Alsulaiman, G. Muhammad, M. A. Bencherif, and M. S. Hossain, "Multilevel weighted feature fusion using convolutional neural networks for EEG motor imagery classification," *IEEE Access*, vol. 7, pp. 18940–18950, 2019.

[109] H. Dose, J. S. Møller, H. K. Iversen, and S. Puthusserypady, "An end-to-end deep learning approach to MI-EEG signal classification for BCIs," *Expert Syst. Appl.*, vol. 114, pp. 532–542, 2018.

[110] Z. Tang, C. Li, and S. Sun, "Single-trial EEG classification of motor imagery using deep convolutional neural networks," *Optik (Stuttg).*, vol. 130, pp. 11–18, 2017.

[111] G. Dai, J. Zhou, J. Huang, and N. Wang, "HS-CNN: a CNN with hybrid convolution scale for EEG motor imagery classification," *J. Neural Eng.*, vol. 17, no. 1, p. 16025, 2020.

[112] B.-H. Lee, J.-H. Jeong, and S.-W. Lee, "SessionNet: Feature similarity-based weighted ensemble learning for motor imagery classification," *IEEE Access*, vol. 8, pp. 134524–134535, 2020.

[113] H. Wu *et al.*, "A Parallel Multiscale Filter Bank Convolutional Neural Networks for Motor Imagery EEG Classification," *Front. Neurosci.*, vol. 13, p. 1275, 2019.

[114] C. Zhang, Y.-K. Kim, and A. Eskandarian, "EEG-inception: an accurate and robust end-to-end neural network for EEG-based motor imagery classification," *J. Neural Eng.*, vol. 18, no. 4, p. 46014, 2021.

[115] S. U. Amin, M. Alsulaiman, G. Muhammad, M. A. Mekhtiche, and M. S. Hossain, "Deep Learning for EEG motor imagery classification based on multi-layer CNNs feature fusion," *Futur. Gener. Comput. Syst.*, vol. 101, pp. 542–554, 2019.

[116] M. Xu *et al.*, "Learning EEG topographical representation for classification via convolutional neural network," *Pattern Recognit.*, vol. 105, p. 107390, 2020.

[117] J. J. Liao, J. J. Luo, T. Yang, R. Q. Y. So, and M. C. H. Chua, "Effects of local and global spatial patterns in EEG motor-imagery classification using convolutional neural network," *Brain-Computer Interfaces*, vol. 7, no. 3–4, pp. 47–56, 2020.

[118] M.-A. Li, J.-F. Han, and L.-J. Duan, "A Novel MI-EEG Imaging With the Location Information of Electrodes," *IEEE Access*, vol. 8, pp. 3197–3211, 2019.

[119] D. F. Collazos-Huertas, A. M. Álvarez-Meza, C. D. Acosta-Medina, G. A. Castaño-Duque, and G. Castellanos-Dominguez, "CNN-based framework using spatial dropping for enhanced interpretation of neural activity in motor imagery classification," *Brain Informatics*, vol. 7, no. 1, pp. 1–13, 2020.

[120] Y. Hou, L. Zhou, S. Jia, and X. Lun, "A novel approach of decoding EEG four-class motor imagery tasks via scout ESI and CNN," *J. Neural Eng.*, vol. 17, no. 1, p. 16048, 2020.

[121] X. Liu, Y. Shen, J. Liu, J. Yang, P. Xiong, and F. Lin, "Parallel Spatial–Temporal Self-Attention CNN-Based Motor Imagery Classification for BCI," *Front. Neurosci.*, vol. 14, 2020.

[122] S. U. Amin, H. Altaheri, G. Muhammad, M. Alsulaiman, and W. Abdul, "Attention based Inception model for robust EEG motor imagery classification," in *2021 IEEE International Instrumentation and Measurement Technology Conference (I2MTC)*, 2021, pp. 1–6.

[123] X. Zhu, P. Li, C. Li, D. Yao, R. Zhang, and P. Xu, "Separated channel convolutional neural network to realize the training free motor imagery BCI systems," *Biomed. Signal Process. Control*, vol. 49, pp. 396–403, 2019.

[124] Y. K. Musallam *et al.*, "Electroencephalography-based motor imagery classification using temporal convolutional network fusion," *Biomed. Signal Process. Control*, vol. 69, p. 102826, 2021.

[125] M. Riyad, M. Khalil, and A. Adib, "MI-EEGNET: A novel convolutional neural network for motor imagery classification," *J. Neurosci. Methods*, vol. 353, p. 109037, 2021.

[126] D. Li, J. Wang, J. Xu, and X. Fang, "Densely feature fusion based on convolutional neural networks for motor imagery EEG classification," *IEEE Access*, vol. 7, pp. 132720–132730, 2019.

[127] K.-W. Ha and J.-W. Jeong, "Temporal Pyramid Pooling for Decoding Motor-Imagery EEG Signals," *IEEE Access*, vol. 9, pp. 3112–3125, 2021.

[128] K. Zhang, N. Robinson, S.-W. Lee, and C. Guan, "Adaptive transfer learning for EEG motor imagery classification with deep Convolutional Neural Network," *Neural Networks*, vol. 136, pp. 1–10, 2021.

[129] H. Zhao, Q. Zheng, K. Ma, H. Li, and Y. Zheng, "Deep Representation-Based Domain Adaptation for Nonstationary EEG Classification," *IEEE Trans. Neural Networks Learn. Syst.*, 2020.

[130] G. Xu *et al.*, "A deep transfer convolutional neural network framework for EEG signal classification," *IEEE Access*, vol. 7, pp. 112767–112776, 2019.

[131] C. Brunner, R. Leeb, G. Müller-Putz, A. Schlögl, and G. Pfurtscheller, "BCI Competition 2008–Graz data set A," *Inst. Knowl. Discov. Graz Univ. Technol.*, vol. 16, pp. 1–6, 2008.

[132] H. Cho, M. Ahn, S. Ahn, M. Kwon, and S. C. Jun, "EEG datasets for motor imagery brain–computer interface," *Gigascience*, vol. 6, no. 7, p. gix034, 2017.

[133] B. Blankertz, G. Dornhege, M. Krauledat, K.-R. Müller, and G. Curio, "The non-invasive Berlin brain–computer interface: fast acquisition of effective performance in untrained subjects," *Neuroimage*, vol. 37, no. 2, pp. 539–550, 2007.

[134] D. P. Kingma and M. Welling, "Auto-encoding variational bayes," *arXiv Prepr. arXiv1312.6114*, 2013.

[135] Y. Li, X.-R. Zhang, B. Zhang, M.-Y. Lei, W.-G. Cui, and Y.-Z.

Guo, “A channel-projection mixed-scale convolutional neural network for motor imagery EEG decoding,” *IEEE Trans. Neural Syst. Rehabil. Eng.*, vol. 27, no. 6, pp. 1170–1180, 2019.

[136] B. Blankertz *et al.*, “The BCI competition III: Validating alternative approaches to actual BCI problems,” *IEEE Trans. neural Syst. Rehabil. Eng.*, vol. 14, no. 2, pp. 153–159, 2006.

[137] L. Wang, W. Huang, Z. Yang, and C. Zhang, “Temporal-spatial-frequency depth extraction of brain-computer interface based on mental tasks,” *Biomed. Signal Process. Control*, vol. 58, p. 101845, 2020.

[138] D. Freer and G.-Z. Yang, “Data augmentation for self-paced motor imagery classification with C-LSTM,” *J. Neural Eng.*, vol. 17, no. 1, p. 16041, 2020.

[139] A. L. Goldberger *et al.*, “PhysioBank, PhysioToolkit, and PhysioNet: components of a new research resource for complex physiologic signals,” *Circulation*, vol. 101, no. 23, pp. e215–e220, 2000.

[140] L. Xiaoling, “Motor imagery-based EEG signals classification by combining temporal and spatial deep characteristics,” *Int. J. Intell. Comput. Cybern.*, 2020.

[141] K. Zhang *et al.*, “Instance transfer subject-dependent strategy for motor imagery signal classification using deep convolutional neural networks,” *Comput. Math. Methods Med.*, vol. 2020, 2020.

[142] P. Ofner, A. Schwarz, J. Pereira, and G. R. Müller-Putz, “Upper limb movements can be decoded from the time-domain of low-frequency EEG,” *PLoS One*, vol. 12, no. 8, p. e0182578, 2017.

[143] J. Chen, Z. Yu, Z. Gu, and Y. Li, “Deep Temporal-Spatial Feature Learning for Motor Imagery-Based Brain–Computer Interfaces,” *IEEE Trans. Neural Syst. Rehabil. Eng.*, vol. 28, no. 11, pp. 2356–2366, 2020.

[144] D. Steyrl, R. Scherer, O. Förstner, and G. R. Müller-Putz, “Motor imagery brain-computer interfaces: random forests vs regularized LDA-non-linear beats linear,” in *Proceedings of the 6th International Brain-Computer Interface Conference*, 2014, pp. 241–244.

[145] X. Ma, S. Qiu, and H. He, “Multi-channel EEG recording during motor imagery of different joints from the same limb,” *Sci. data*, vol. 7, no. 1, pp. 1–9, 2020.

[146] H. K. Lee and Y.-S. Choi, “Application of continuous wavelet transform and convolutional neural network in decoding motor imagery brain-computer interface,” *Entropy*, vol. 21, no. 12, p. 1199, 2019.

[147] C. J. Ortiz-Echeverri, S. Salazar-Colores, J. Rodríguez-Reséndiz, and R. A. Gómez-Loenzo, “A new approach for motor imagery classification based on sorted blind source separation, continuous wavelet transform, and convolutional neural network,” *Sensors*, vol. 19, no. 20, p. 4541, 2019.

[148] S. Chaudhary, S. Taran, V. Bajaj, and A. Sengur, “Convolutional neural network based approach towards motor imagery tasks EEG signals classification,” *IEEE Sens. J.*, vol. 19, no. 12, pp. 4494–4500, 2019.

[149] X.-L. Tang, W.-C. Ma, D.-S. Kong, and W. Li, “Semisupervised deep stacking network with adaptive learning rate strategy for motor imagery EEG recognition,” *Neural Comput.*, vol. 31, no. 5, pp. 919–942, 2019.

[150] Z. Zhang *et al.*, “A novel deep learning approach with data augmentation to classify motor imagery signals,” *IEEE Access*, vol. 7, pp. 15945–15954, 2019.

[151] X. Tang, N. Zhang, J. Zhou, and Q. Liu, “Hidden-layer visible deep stacking network optimized by PSO for motor imagery EEG recognition,” *Neurocomputing*, vol. 234, pp. 1–10, 2017.

[152] L. Deng, Jia and Dong, Wei and Socher, Richard and Li, Li-Jia and Li, Kai and Fei-Fei, “Imagenet: A large-scale hierarchical image database,” in *IEEE Conference on Computer Vision and Pattern Recognition*, 2009, pp. 248–255.

[153] H. Altaheri, M. Alsulaiman, G. Muhammad, S. U. Amin, M. Bencherif, and M. Mekhtiche, “Date fruit dataset for intelligent harvesting,” *Data Br.*, vol. 26, p. 104514, Oct. 2019.

[154] M. Alsulaiman, G. Muhammad, M. A. Bencherif, A. Mahmood, and Z. Ali, “KSU rich Arabic speech database,” *Inf.*, vol. 16, no. 6 B, pp. 4231–4253, 2013.

[155] Graz University of Technology, “Data sets - BNCI Horizon 2020.” [Online]. Available: http://bnci-horizon-2020.eu/database/data-sets. [Accessed: 05-Feb-2021].

[156] F. Lotte, “Fabien Lotte’s professional homepage - Links.” [Online]. Available: https://sites.google.com/site/fabienlotte/bci-community/links?authuser=0#h.p_ID_172. [Accessed: 05-Feb-2021].

[157] R. Scherer *et al.*, “Individually adapted imagery improves brain-computer interface performance in end-users with disability,” *PLoS One*, vol. 10, no. 5, p. e0123727, 2015.

[158] M. Kaya, M. K. Binli, E. Ozbay, H. Yanar, and Y. Mishchenko, “A large electroencephalographic motor imagery dataset for electroencephalographic brain computer interfaces,” *Sci. data*, vol. 5, p. 180211, 2018.

[159] N. Brodu, F. Lotte, and A. Lécuyer, “Exploring two novel features for EEG-based brain–computer interfaces: Multifractal cumulants and predictive complexity,” *Neurocomputing*, vol. 79, pp. 87–94, 2012.

[160] A. Ramos-Murguialday *et al.*, “Brain–machine interface in chronic stroke rehabilitation: a controlled study,” *Ann. Neurol.*, vol. 74, no. 1, pp. 100–108, 2013.

[161] X. Zhang, L. Yao, Q. Z. Sheng, S. S. Kanhere, T. Gu, and D. Zhang, “Converting your thoughts to texts: Enabling brain typing via deep feature learning of eeg signals,” in *2018 IEEE international conference on pervasive computing and communications (PerCom)*, 2018, pp. 1–10.

[162] J. Van Erp, F. Lotte, and M. Tangermann, “Brain-computer interfaces: beyond medical applications,” *Computer (Long. Beach. Calif).*, vol. 45, no. 4, pp. 26–34, 2012.

[163] R. Yuste *et al.*, “Four ethical priorities for neurotechnologies and AI,” *Nat. News*, vol. 551, no. 7679, p. 159, 2017.

[164] K. LaFleur, K. Cassady, A. Doud, K. Shades, E. Rogin, and B. He, “Quadcopter control in three-dimensional space using a noninvasive motor imagery-based brain–computer interface,” *J. Neural Eng.*, vol. 10, no. 4, p. 46003, 2013.

[165] Y. Yu *et al.*, “Toward brain-actuated car applications: Self-paced control with a motor imagery-based brain-computer interface,” *Comput. Biol. Med.*, vol. 77, pp. 148–155, 2016.

[166] X. Zhang, L. Yao, C. Huang, Q. Z. Sheng, and X. Wang, “Intent recognition in smart living through deep recurrent neural networks,” in *International Conference on Neural Information Processing*, 2017, pp. 748–758.

[167] T. Li, J. Zhang, T. Xue, and B. Wang, “Development of a novel motor imagery control technique and application in a gaming environment,” *Comput. Intell. Neurosci.*, vol. 2017, 2017.

[168] A. Kreilinger, H. Hiebel, and G. R. Müller-Putz, “Single versus multiple events error potential detection in a BCI-controlled car game with continuous and discrete feedback,” *IEEE Trans. Biomed. Eng.*, vol. 63, no. 3, pp. 519–529, 2015.

[169] X. Zhang, L. Yao, S. S. Kanhere, Y. Liu, T. Gu, and K. Chen, “Mindid: Person identification from brain waves through attention-based recurrent neural network,” *Proc. ACM Interactive, Mobile, Wearable Ubiquitous Technol.*, vol. 2, no. 3, pp. 1–23, 2018.

[170] X. Zhang, L. Yao, C. Huang, T. Gu, Z. Yang, and Y. Liu, “DeepKey: An EEG and gait based dual-authentication system,” *arXiv Prepr. arXiv1706.01606*, 2017.